

RESEARCH ARTICLE

[View Article Online](#)  
[View Journal](#)



Cite this: DOI: 10.1039/d5qi02023a

## Unsupported gallatabenzene via rare-earth-metal pentadienyl complexes

Jakob Lebon, Manfred Manßen, Cäcilia Maichle-Mössmer, Peter Sirsch \* and Reiner Anwander \*

The treatment of rare-earth-metal aluminata/gallata complexes with the Lewis acids  $\text{AlMe}_3$  and  $\text{ECl}_3$  ( $\text{E} = \text{Al, Ga}$ ) gives access to new group 13 metallacyclic fragments. The reaction of the mixed ytrocene  $(\text{C}_5\text{Me}_5)\text{Y}(\mu\text{-Me})(\text{AlC}_5\text{H}_3\text{Me-1-tBu}_2\text{-3,5})$  with  $\text{AlMe}_3$  produced the bis(heteroaluminato) complex  $(\text{C}_5\text{Me}_5)\text{Y}[(3,5\text{-tBu}_2\text{C}_5\text{H}_3\text{AlMe}_2)(\text{AlMe}_3)]$ . The reaction of  $(\text{C}_5\text{Me}_5)\text{Y}(\mu\text{-Me})(\text{AlC}_5\text{H}_3\text{Me-1-tBu}_2\text{-3,5})$  with  $\text{AlCl}_3$  gave an organoaluminium entity with a central chair conformation of alternating aluminium and carbon atoms. Alternatively, the new  $\text{Al}_3$  entity can be interpreted as a monoanionic aluminatabenzene moiety  $[(1\text{-Me-3,5-tBu}_2\text{C}_5\text{H}_3\text{Al})(\text{THF})]$ , which is stabilized by the cationic dialuminium fragment  $[3,5\text{-tBu}_2\text{C}_5\text{H}_3(\text{AlMe}_2)]$ . The donor (THF) free  $\text{Ga}_3$  homologue was obtained from bis(gallata) "open" lutocene  $(1\text{-Me-3,5-tBu}_2\text{C}_5\text{H}_3\text{Ga})(\mu\text{-Me})\text{Lu}(1\text{-Me-3,5-tBu}_2\text{C}_5\text{H}_3\text{Ga})$  and  $\text{GaCl}_3$ . The reaction of the bis(gallata) lutetium sandwich complex with  $\text{KOtBu}$  gave the potassium coordination polymer  $[\text{K}(1\text{-Me-3,5-tBu}_2\text{C}_5\text{H}_3\text{Ga})(\text{THF})]_n$ , which can be converted to the separated ion pair  $[(1\text{-Me-3,5-tBu}_2\text{C}_5\text{H}_3\text{Ga})][\text{K}[[2.2.2]\text{crypt}]]$  by addition of the [2.2.2]cryptand. The isolated compounds were analyzed by  $^1\text{H}$ ,  $^{13}\text{C}$ ,  $^{89}\text{Y}$ , and variable temperature  $^1\text{H}$  NMR spectroscopy, SC-XRD, IR spectroscopy, and elemental analysis. The bonding of the unsupported gallatabenzene moiety was further investigated by DFT calculations.

Received 3rd October 2025,  
Accepted 3rd December 2025  
DOI: 10.1039/d5qi02023a  
[rsc.li/frontiers-inorganic](http://rsc.li/frontiers-inorganic)

## Introduction

The chemistry of 5- and 6-membered heterocycles of the heavier group 13 and 14 elements – and more specifically the analysis of their aromatic behaviour – is an ongoing topic in main group chemistry.<sup>1</sup> For the group 14 elements silicon and germanium, both the dianionic heterocyclopentadienediides and the neutral sila- and germabzenes were first synthesized several decades ago and feature well-understood structural motifs (Chart 1).<sup>2–6</sup> In the case of the heavier group 13 elements, the variety of 5- and 6-membered heterocycles is far more limited.<sup>7–14</sup> While alumoles and galloles and their dianionic structures have been investigated for a longer period (Chart 1),<sup>7–10</sup> the advances in the chemistry of the monoanionic heterobenzene congeners have remained modest.<sup>11–14</sup> Even though work in the field of group 13 element heterobenzenes has been highlighted by the gallatabenzene manganese complex by Ashe in 1995,<sup>11</sup> it was further exploited only 20 years later by Yamashita.<sup>12–14</sup> The Yamashita group described a series of transition metal heterobenzene complexes, including the first ion-separated lithium aluminata (A)- and gallata-

benzenes (B). Focus was also put on the extent of aromatic bonding in such monoanionic metallacycles.<sup>11–14</sup> In our previous work, we utilized a di-tBu-substituted pentadienyl ligand (dtbp,  $\text{C}_5\text{H}_3\text{tBu}_2\text{-3,5}$ )<sup>15</sup> to access rare-earth metal aluminata- and gallatabenzene complexes, including the (mixed) sandwich methyl complexes  $(\text{C}_5\text{Me}_5)\text{Y}(\mu\text{-Me})(\text{AlC}_5\text{H}_3\text{Me-1-tBu}_2\text{-3,5})$  and  $(1\text{-Me-3,5-tBu}_2\text{C}_5\text{H}_3\text{Ga})(\mu\text{-Me})\text{Lu}(1\text{-Me-3,5-tBu}_2\text{C}_5\text{H}_3\text{Ga})$ .<sup>16,17</sup>

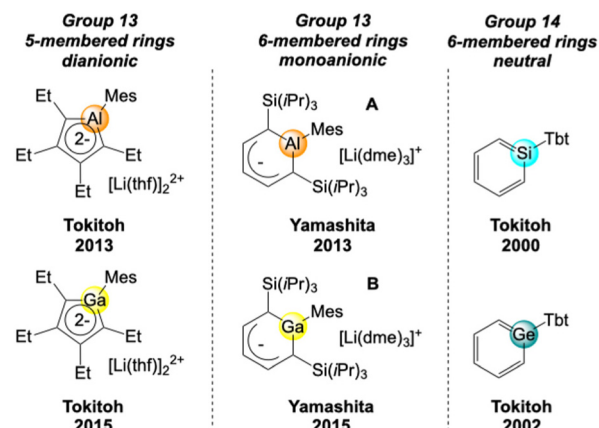


Chart 1 Milestones in the development of group 13 heterocyclopentadienediides<sup>7,10</sup> and group 13/14 heterobenzenes (Tbt = 2,4,6-tris(trimethylsilyl)methylphenyl).<sup>2,3,12,13</sup>

Institut für Anorganische Chemie, Eberhard Karls Universität Tübingen,  
Auf der Morgenstelle 18, 72076 Tübingen, Germany.  
E-mail: [reiner.anwander@uni-tuebingen.de](mailto:reiner.anwander@uni-tuebingen.de)



While the formation of such heterobenzene-type ligands at small- to medium-sized rare-earth metals (Lu, Y) was easily achieved, a conceivable salt-metathesis route utilizing K(2,4-dtbp) and compounds  $\text{EClMe}_2$  ( $\text{E} = \text{Al, Ga}$ ) to access unsupported metallacycles has been unsuccessful so far. Here, we describe that an ion-separated potassium gallatabenzene can be ultimately obtained by betting on the oxophilicity of rare-earth metals.

## Results and discussion

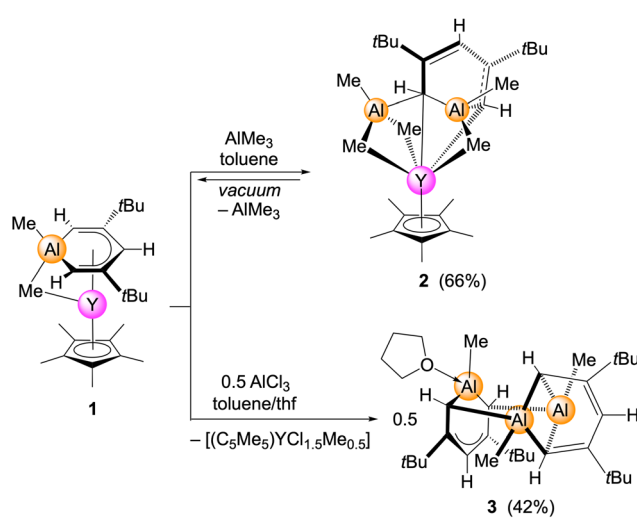
### Reactivity of $(\text{C}_5\text{Me}_5)\text{Y}(\mu\text{-Me})(\text{AlC}_5\text{H}_3\text{Me-1-}t\text{Bu}_2\text{-3,5})$ (1) towards $\text{AlMe}_3$ and $\text{AlCl}_3$

Previous derivatization reactions of the half-open sandwich complexes  $(1\text{-Me-3,5-}t\text{Bu}_2\text{-C}_5\text{H}_3\text{E})(\mu\text{-Me})\text{Y}(2,4\text{-dtbp})$  ( $\text{E} = \text{Al, Ga}$ ) revealed that the coordination capability of the 2,4-dtbp ligand is significantly enhanced *via* cyclometallation.<sup>18</sup> For example, the open pentadienyl ligand is easily displaced by penta-methylcyclopentadienyl to afford the mixed ytrocene  $(\text{C}_5\text{Me}_5)\text{Y}(\mu\text{-Me})(\text{AlC}_5\text{H}_3\text{Me-1-}t\text{Bu}_2\text{-3,5})$  (1).<sup>17</sup> It was also revealed that the coordination strength of the aluminata/gallatabenzene ligands is additionally promoted by a strong interaction of the ring group 13 element with the methyl group bridging to the rare-earth-metal centre.<sup>16,17</sup> The bridging methyl group could neither be cleaved by donor molecules nor be abstracted *via* the use of trityl borate  $[\text{CPh}_3][\text{B}(\text{C}_6\text{F}_5)_4]$ .<sup>16,17</sup> We assumed that a reactivity study involving competitive Lewis acids might give further insights into the stability of the  $[\text{Y}(\mu\text{-Me})(\text{AlC}_5\text{H}_3\text{Me-1-}t\text{Bu}_2\text{-3,5})]$  fragment. Therefore, the  $\text{C}_5\text{Me}_5$ -supported aluminatabenzene complex 1 was treated with the strong Lewis acids  $\text{AlMe}_3$  and  $\text{AlCl}_3$ . The  $\text{AlMe}_3$  reaction resulted in heteroaluminato formation across the dianionic aluminatabenzene ligand and the formation of the trimetallic complex  $(\text{C}_5\text{Me}_5)\text{Y}[(3,5\text{-}t\text{Bu}_2\text{C}_5\text{H}_3\text{AlMe}_2)(\text{AlMe}_3)]$  (2, Scheme 1). Although complex 2 can be readily reproduced and isolated as single crystals, it

decomposes under vacuum to precursor 1 and  $\text{AlMe}_3$ , impeding its isolation as a solid bulk material.

As revealed by a single-crystal X-ray diffraction (SC-XRD) analysis, the pentadienyl backbone of compound 2 displays conjugated localized double bonds ( $\text{C}2=\text{C}3$  and  $\text{C}4=\text{C}5$ ). Overall, the molecular structure of 2 is reminiscent of the half-sandwich bis(aluminato)  $(\text{C}_5\text{Me}_5)\text{Y}(\text{AlMe}_4)_2$ ,<sup>19</sup> referring to the quite symmetric coordination of the  $\text{AlR}_4$  fragments to the yttrium centre (Fig. 1/top). The  $\text{Y}\cdots\text{Al}$  distances (2.7999(6) and 2.8233(5) Å) in 2 are shorter than those in  $(\text{C}_5\text{Me}_5)\text{Y}(\text{AlMe}_4)_2$  (2.9257(7) and 3.1112(7) Å), while the  $\text{Y}-\text{C}$  distances (2.5144(17) and 2.8095(17) Å) are in the range of those detected for  $(\text{C}_5\text{Me}_5)\text{Y}(\text{AlMe}_4)_2$  (2.549(3)–2.655(3) Å).<sup>19</sup>

In contrast, the tetracyclic  $\text{Al}_3$  species  $[(1\text{-Me-3,5-}t\text{Bu}_2\text{-C}_5\text{H}_3\text{Al})(\text{THF})][3,5\text{-}t\text{Bu}_2\text{-C}_5\text{H}_3(\text{AlMe})_2]$  (3), resulting from the  $\text{AlCl}_3$  reaction, was isolated as thermally stable crystals. The formation of 3 seems mainly driven by the co-formation of two equiv. of the mostly chlorinated half-sandwich species  $[(\text{C}_5\text{Me}_5)\text{YCl}_{1.5}\text{Me}_{0.5}]$ , which could be separated *via* extraction of 3 with *n*-pentane and verified from the residue as the metathesis products  $(\text{C}_5\text{Me}_5)\text{YCl}(\text{THF})$  and  $[(\text{C}_5\text{Me}_5)\text{YCl}_{1.5}\text{Me}_{0.5}]$  *via* proton NMR spectroscopy and SC-XRD.<sup>20</sup> Compound 3 features a multi-metallacyclic structure (Fig. 1). One cycle comprises the atoms  $\text{Al3-C1-C2-C3-C4-C5}$  forming a 6-membered monoanionic fragment. Compared to precursor 1, this 6-mem-



**Scheme 1** Synthesis of half-sandwich heteroaluminato 2 and tetracyclic  $\text{Al}_3$  compound 3.

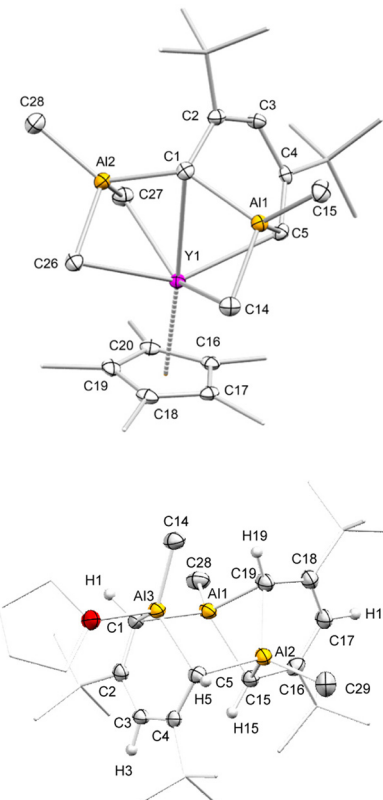


**Fig. 1** Crystal structures of 2 (top) and 3 (bottom), with ellipsoids set at 50%. For 2, all hydrogen atoms and for 3, methyl hydrogen atoms have been omitted for clarity. For selected interatomic distances, see the SI.



bered ring displays minor deviations of the C–C distances (1.407(4)–1.428(4) Å) and shorter Al–C<sub>ring</sub> distances (1.961(3) and 1.980(3) Å) (**1**: C–C 1.376(3)–1.446(3); Al–C<sub>ring</sub> 2.016(3) and 2.019(3) Å). The second and third cycles incorporate a second pentadienyl backbone, expanding the formal 6-membered cycle by another AlMe fragment, in a lid-like structure. This structural motif can be interpreted as a pentadienyl stabilized “bisalumocyclobutane” cation. The second cycle, which involves the atoms  $\mu$ -Al1–C19–C18–C17–C16–C15– $\mu$ -Al2, displays more localized, but conjugated double bonds with C–C interatomic distances ranging from 1.389(4) Å to 1.427(4) Å. The high-valent bonding situation of carbon atom C15 led to the conclusion that compound **3** is a zwitterionic compound composed of a monoanionic aluminatabenzene moiety (**I**<sub>b</sub>, Scheme 2) and an Al<sub>2</sub> cationic fragment (**I**<sub>c</sub>, Scheme 2). The third cycle, featuring the “bisalumocyclobutane” moiety Al1–C19–Al2–C15, displays a hitherto unknown organoaluminium structural pattern, with common Al–C distances (2.027(3)–2.042(3) Å). Furthermore, the Al1–Al2 distance of 2.6810(14) Å does not indicate any metal–metal interaction. The aluminium atoms of the “bisalumocyclobutane” moiety connect to the *ortho*-C atoms of the aluminatabenzene moiety with usual Al–C distances (2.072(3) and 2.071(3) Å).

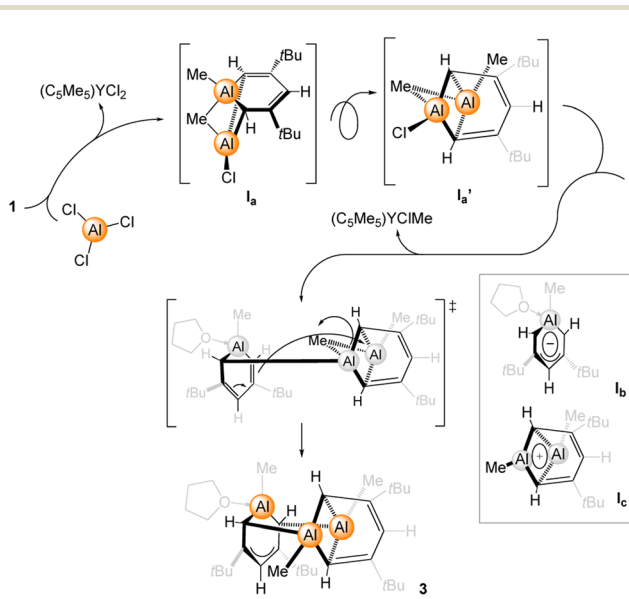
For comparison, fused-ring tricyclic organoaluminium species featuring a 4-membered Al–C–Al–C were obtained from hydroalumination of di(*tert*-butyl)butadiyne with dimethylaluminium hydride.<sup>21,22</sup> Furthermore, similar 4-membered metallacycles were also detected in a heptacyclic species originating from the reaction of EX<sub>3</sub> (E = Al and Ga) with the tri-lithium compound 1,3-[PhMe<sub>2</sub>Si–C(Li)=C(H)]<sub>2</sub>C<sub>6</sub>H<sub>3</sub>Li.<sup>23</sup> Fully separated organoaluminium ion pairs include the structurally

characterized compounds [Me<sub>2</sub>Al(15-crown-5)][Me<sub>2</sub>AlCl<sub>2</sub>] and [tBu<sub>2</sub>Al(tmada)][tBu<sub>2</sub>AlBr<sub>2</sub>].<sup>24,25</sup>

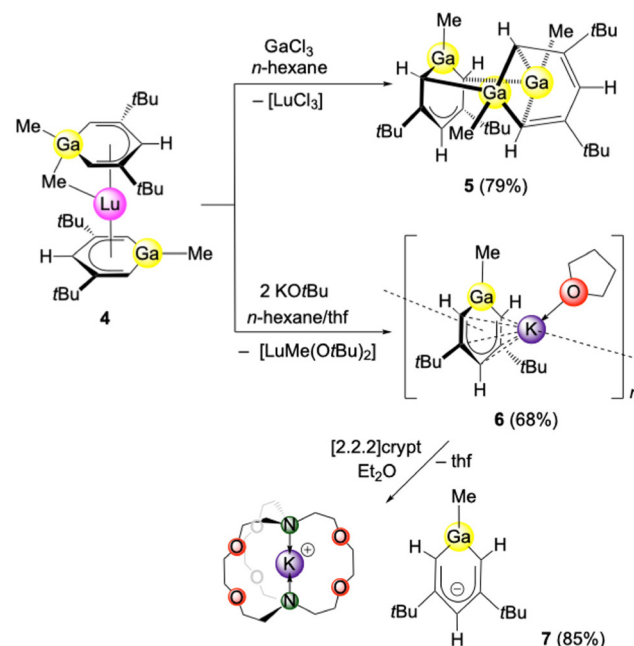
Since we were able to isolate the side product [(C<sub>5</sub>Me<sub>5</sub>)YCl<sub>1.5</sub>Me<sub>0.5</sub>] and could revert to complex **2** for initiating the reaction step/path, the following reaction mechanism for the formation of compound **3** can be proposed (Scheme 2). Accordingly, complex **1** readily reacts with AlCl<sub>3</sub> forming [(C<sub>5</sub>Me<sub>5</sub>)YCl<sub>2</sub>] and intermediate **I**<sub>a</sub>. By changing the perspective of **I**<sub>a</sub> to **I**<sub>a'</sub>, it is apparent that the displacement of the remaining chlorido by another equivalent of **1** can take place, with the cationic part being already in place. Thus, *via* exchange of the chlorido against the monoanionic aluminatabenzene ligand and elimination of [(C<sub>5</sub>Me<sub>5</sub>)YClMe], a formal anion (**I**<sub>b</sub>)–cation (**I**<sub>c</sub>) combination may lead to the isolation of **3**. To further prove the overall ionic nature of **3**, its fragmentation pattern was investigated by mass spectrometry. By using mild ionization methods at ambient temperature, the dominant peak obtained *via* the electron ionization method was identified as the cationic fragment **I**<sub>c</sub>. Other smaller signals could be referred to as compound **3** and 3-THF-CH<sub>3</sub>.

### Reactivity of bis(gallatabenzene) lutetocene (1-Me-3,5-tBu<sub>2</sub>-C<sub>5</sub>H<sub>3</sub>Ga)( $\mu$ -Me)Lu(1-Me-3,5-tBu<sub>2</sub>-C<sub>5</sub>H<sub>3</sub>Ga) (**4**) towards GaCl<sub>3</sub> and KOtBu

Since gallium forms more covalent Ga–C bonds, the respective abstraction of a gallatabenzene moiety from a rare-earth-metal complex should increase the feasibility of ion fragmentation in solution. Therefore, we examined the corresponding reactivity of the previously published and fully characterized bis(gallatabenzene) lutetium sandwich complex (1-Me-3,5-tBu<sub>2</sub>-C<sub>5</sub>H<sub>3</sub>Ga)



**Scheme 2** Proposed mechanistic pathway for the formation of compound **3**. Aluminatabenzene **1** reacts with AlCl<sub>3</sub> to form the intermediate **I**<sub>a</sub> or **I**<sub>a'</sub> (different perspectives) and [(C<sub>5</sub>Me<sub>5</sub>)YCl<sub>2</sub>]. Further reaction with a second equivalent of **1** proceeds *via* the formation of [(C<sub>5</sub>Me<sub>5</sub>)YClMe] and complex **3** possibly involving a cation–anion addition.



**Scheme 3** Metathetical synthesis of Ga<sub>3</sub> compound **5** and polymeric potassium salt **6**, which can be converted to ion-separated complex **7** *via* addition of cryptand.



$(\mu\text{-Me})\text{Lu}(1\text{-Me-3,5-}t\text{Bu}_2\text{-C}_5\text{H}_3\text{Ga})$  (**4**, Scheme 3).<sup>17</sup> Gratifyingly, the  $\text{GaCl}_3$  reaction gave compound  $[(1\text{-Me-3,5-}t\text{Bu}_2\text{-C}_5\text{H}_3\text{Ga})_2]$  (**5**) as the THF free heavier homologue of compound **3**. Due to the presence of two gallatabenzene moieties in **4**, compared to the single aluminatabenzene moiety in precursor **1**, the formation of **5** requires only 1 equiv. of  $\text{GaCl}_3$ . Comparing both SC-XRD structures of **3** and **5**, no significant difference is detected in the overall bonding situation. However, the Ga–C and C–C ring distances in compound **5** differ more than expected (Fig. 2). The anionic 6-membered ring moiety involving Ga3–C1–C2–C3–C4–C5 revealed comparatively shorter C–C distances (1.395(6) and 1.399(6) for C2–C3 and C3–C4, respectively), indicating a higher degree of conjugation and aromaticity. This is also reflected in the Ga–C distances (1.946(4) and 1.953(4) Å), which are shorter than the Al–C distances in compound **2**. The Ga–C<sub>ring</sub> distances are comparable to those in the heteroadamantane cluster  $[(\text{GaEt})_6(\text{CET})_4]$  (1.965(4)–1.992(7) Å), obtained *via* hydrogallation of propyne with  $\text{Me}_2\text{GaH}$ ,<sup>26</sup> and in Yamashita's lithium gallatabenzene [ $1\text{-Mes-2,6-Si}(i\text{Pr}_3)_2\text{C}_5\text{H}_3\text{Ga}]Li(\text{dme})$  (1.939(3) and 1.941(3) Å).<sup>13</sup> The metallacycle comprising Ga1–C15–C16–C17–C18–C19 features allylic C–C bonding in the pentadienyl backbone, instead of two conjugated double bonds, with three almost equal C–C distances (1.432(5), 1.401(5) and 1.412(5) Å).

Exploiting the highly oxophilic character of rare-earth metals, gallatabenzene displacement from complex **4** was also achieved by treatment with  $\text{KO}/\text{Bu}$ . Accordingly, the potassium salt  $[(1\text{-Me-3,5-}t\text{Bu}_2\text{-C}_5\text{H}_3\text{Ga})\text{K}(\text{thf})]_n$  (**6**) could be accessed in good yield (Scheme 3, Fig. 3/top). Coordination polymer **6** allows a more detailed view of the bonding situation and potential aromaticity of the gallatabenzene moiety. The gallatabenzene coordination to the potassium entails only a minor distortion of the gallium atom out of the ring plane (0.01 Å). Enhanced participation of the Ga–C bond in the conjugated ring system is further revealed by shorter Ga–C ring distances of 1.895(5) and 1.893(5) Å. For comparison, the terminal Ga–C<sub>methyl</sub> distance measures 1.963 Å. The C–C ring distances range from 1.395(6) to 1.424(6) Å.

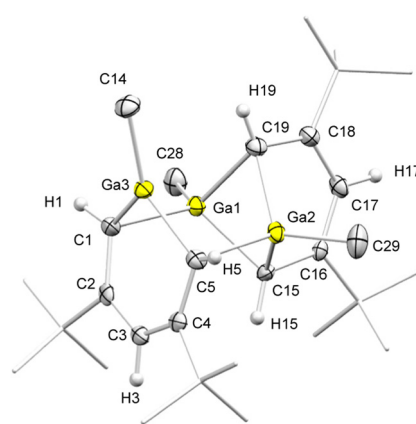


**Fig. 2** Crystal structure of **5**, with ellipsoids set at 50%. Methyl hydrogen atoms have been omitted for clarity. For selected interatomic distances, see the SI.

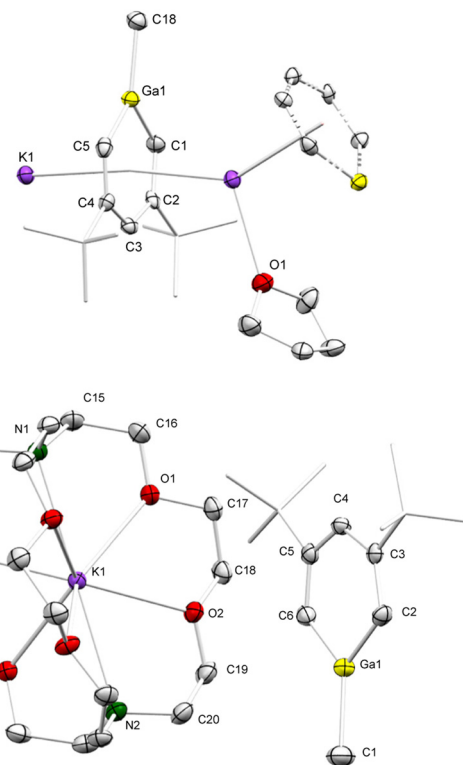


**Fig. 3** Crystal structures of polymer **6** (top, repeat unit) and ion pair **7** (bottom), with ellipsoids set at 50%. All hydrogen atoms have been omitted for clarity. For selected interatomic distances, see the SI.

The <sup>1</sup>H NMR spectrum of compound **6** in  $\text{thf-d}_8$  displays the hydrogen atoms at the C1/C5 (*ortho*) and C3 (*para*) ring positions at lower fields (6.63/5.74 ppm) compared to precursor **4**, corroborating an enhanced aromatic character of the gallatabenzene, despite the coordination of potassium. The K–C<sub>ring</sub> distances in **6** are in the range from 3.095(4) to 3.323(5) Å and the K…Ga distance amounts to 3.4458(11) Å. For further comparison, Yamashita's lithium gallatabenzene [ $1\text{-Mes-2,6-Si}(i\text{Pr}_3)_2\text{C}_5\text{H}_3\text{Ga}]Li(\text{dme})$  exhibits C–C ring and Li–C<sub>ring</sub> distances ranging from 1.396(4) to 1.408(5) Å and from 2.301(7) to 2.702(7) Å, respectively (Li…Ga, 2.931(6) Å).<sup>13</sup> The *meta*- and *para*-ring protons of the lithium gallatabenzene [ $1\text{-Mes-2,6-Si}(i\text{Pr}_3)_2\text{C}_5\text{H}_3\text{Ga}]Li(\text{dme})$  were observed at 8.23 and 6.01 ppm ( $\text{C}_6\text{D}_6$ ), respectively.<sup>13</sup>

To further investigate the feasibility of a metal-unsupported “free” monoanionic gallatabenzene and the effect of potassium coordination on the structure of the 6-membered metallacycle, compound **6** was reacted with [2.2.2]cryptand. As anticipated, potassium encapsulation yielded the separated ion pair  $[(1\text{-Me-3,5-}t\text{Bu}_2\text{-C}_5\text{H}_3\text{Ga})][\text{K}[[2.2.2]\text{crypt}]]$  (**7**) (Scheme 3 and Fig. 3/bottom). However, any significant differences in the interatomic distances in complexes **6** and **7** were not observed. The <sup>1</sup>H NMR spectra revealed slightly distinct chemical shifts for the ring protons. Accordingly, the ring protons of **6** (6.63/5.74 ppm *versus* 6.41/5.57 ppm in **7**) indicate a higher degree of deshielding caused by the coordinated potassium. The



NMR spectra in  $C_6D_6$  of ion-separated gallatabenzene [1-Mes-2,6-Si(*i*Pr<sub>3</sub>)<sub>2</sub>C<sub>5</sub>H<sub>3</sub>Ga] $[\text{Li}(\text{dme})_3]$  (**B**, Chart 1) were found to be identical to those of gallatabenzene [1-Mes-2,6-Si(*i*Pr<sub>3</sub>)<sub>2</sub>C<sub>5</sub>H<sub>3</sub>Ga] $\text{Li}(\text{dme})$ .<sup>13</sup> This was interpreted in a way that in solution dme dissociates from **B** to give [1-Mes-2,6-Si(*i*Pr<sub>3</sub>)<sub>2</sub>C<sub>5</sub>H<sub>3</sub>Ga] $\text{Li}(\text{dme})$ . Similarly, germanylbenzylpotassium derivatives [(1-*t*Bu-C<sub>5</sub>H<sub>4</sub>Ge)K]<sub>n</sub> (layer structure) and [1-*t*Bu-C<sub>5</sub>H<sub>4</sub>Ge] $[\text{K}([\text{2.2.2}]\text{crypt})]$  revealed very similar <sup>1</sup>H NMR chemical shifts in *thf-d*<sub>8</sub> ( $\Delta\delta \approx 0.2$  ppm), in agreement with ion separation and a fully solvated potassium cation in both solutions.<sup>27</sup> The <sup>13</sup>C resonances of the C1/C5 (*ortho*), C2/C4 (*meta*) and C3 (*para*) ring positions of gallatabenzene [1-Mes-2,6-Si(*i*Pr<sub>3</sub>)<sub>2</sub>C<sub>5</sub>H<sub>3</sub>Ga] $\text{Li}(\text{dme})$  in  $C_6D_6$  were detected at 129.5, 148.2 and 103.0 ppm, respectively.<sup>13</sup> Complexes **6** and **7** revealed the respective <sup>13</sup>C NMR chemical shifts at 97.0/161.7/121.2 ppm and 97.2/159.0/119.7 ppm, respectively. The germanylbenzyl anion in the proposed ion-separated [1-*t*Bu-C<sub>5</sub>H<sub>4</sub>Ge] $[\text{K}(\text{thf})_3]$  displayed the <sup>13</sup>C resonances of the ring carbon atoms at 203.7 (C1/*ortho*), 130.1 (C2/*meta*), 112.9 (C3/*para*), 128.4 (C4/*meta*) and 171.2 (C1/*ortho*),<sup>27</sup> which slightly shifted upfield compared to its neutral germabenzene precursor (*cf.*, Chart 1).

At this point, a more detailed comparison of the monoanionic gallatabenzene moiety of **7** to Yamashita's unsupported monoanionic gallatabenzene **B** (Chart 1) seems expedient. Both compounds clearly differ with respect to synthesis and ring substitution. Briefly, gallatabenzene **B** was obtained from an aluminacyclohexadiene with  $\text{GaCl}_3$  involving metal exchange and subsequent reaction of the gallacyclohexadiene with mesyllithium and finally DME.<sup>13</sup> The aluminacyclohexadiene was accessed from a bis(tri-*isopropylsilyl*)diyne by subsequent treatment with  $\text{HAl}/\text{Bu}_2$ ,  $n\text{Bu}_2\text{SnCl}_2$  and pyridine (for structural drawings, see Chart 1).<sup>12</sup> Consequently, gallatabenzene **B** displays an *ortho* silyl substitution, while ours bears *tert*-butyl substituents in the *meta* position (Fig. 4).

As shown in Fig. 4, the crystal structures of **7** and **B** reveal slightly different bond lengths within the ring moieties. For **7**, they seem to indicate a strengthening of the Ga-C bonds, relative to **B**, and a shortening of the bonds between the carbon atoms in *ortho* and *meta* positions, at the cost of the C(*meta*)-C(*para*) bonds, which are elongated.

## DFT calculations

To gain more insight into the nature of the bonding within these substituted gallatabenzene moieties, we carried out DFT calculations at the B3LYP/6-311++G(d,p) level of theory,<sup>28</sup> followed by a natural bond orbital (NBO) analysis.<sup>29</sup> In a previous study,<sup>17b</sup> the bonding in a DFT model system for a nonsubstituted monoanionic gallatabenzene was analysed and found to be very similar to the one reported earlier by Yamashita for **B**.<sup>13</sup> Accordingly, the bonding in the heterocycle is characterized by polar Ga-C  $\sigma$  bonds and a partial delocalization of  $\pi$  electron density from the ring carbon atoms into the vacant p orbital on Ga. Here, we wanted to investigate in more detail, whether the alkyl and silyl substituents in both systems also affect the bonding within the gallatabenzene ring, as suggested by the respective X-ray structures (see above).

Interestingly, in the crystal structure of **7**, the *tert*-butyl substituents are oriented in different ways, where one C-Me bond in each case is almost aligned with the ring plane, but both are pointing in opposite directions (see Fig. 3). A DFT-optimized geometry for **7** confirmed this arrangement and also revealed an asymmetric bonding within the ring moiety: interatomic distances on the left- and right-hand sides of the ring differed slightly, within a range of 0.01–0.02 Å (for details, see the SI). In the crystal structure of **7**, this is not clearly discernible, due to experimental noise and a minor disorder for one of the substituents. The small differences in bond length can be attributed to the unequal conformation of the substituents. This is corroborated by a model system, where both substituents are related by mirror symmetry, and consequently, all respective distances are equal (for details, see the SI). While at first sight these observations might seem insignificant, they help rationalize the aforementioned bond differences between **7** and **B**, which are in a similar range (see Fig. 4). Accordingly, hyperconjugative interactions involving the alkyl and silyl substituents, respectively, might be the cause for these differences.

To identify hyperconjugation, the NBO approach was shown to be ideally suited.<sup>30</sup> Against this background, we reoptimized the DFT geometry of a model system for the gallatabenzene moiety of **B** and analysed the bonding in both **7** and **B** using NBO methods. A range of geminal and vicinal hyperconjugative interactions within the heterocycle could be identified for **B**, some of them also involving the silyl substituents. Two of the latter are displayed in Fig. 5 (for further details, see the SI). They represent the transfer of electron density from a Ga-C  $\sigma$  bond and a C-C  $\pi$  bond, respectively, to anti-bonding Si-C  $\sigma^*$  orbitals, therefore contributing to the weakening and elongation of the involved bonds.

For **7**, a different set of hyperconjugative interactions was found. They were smaller in number and, in general, somewhat weaker than those for **B**. Additionally, the geometries of two other model systems were optimized, in which the silyl and alkyl substituents, respectively, were moved from the *ortho* to the *meta* position or *vice versa* (for details, see the SI). The results indicated that the position of the substitution is at

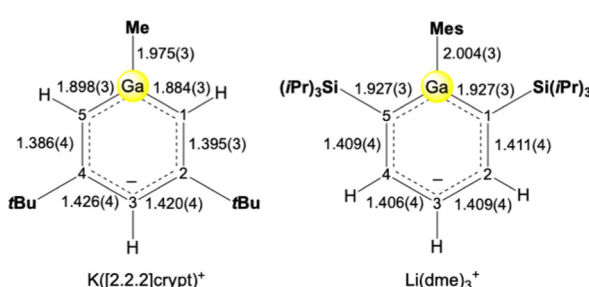
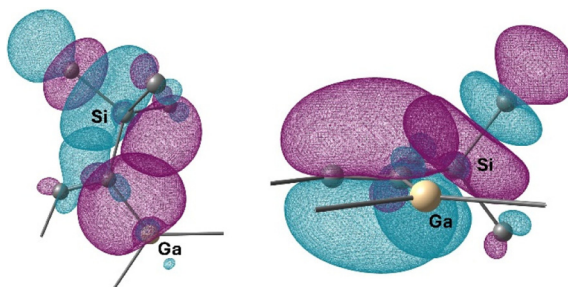


Fig. 4 Comparison of the interatomic Ga-C and C-C ring distances of the two known unsupported gallatabenzenes **7** (left, this work) and **B** (right).<sup>13</sup> Ring carbon atoms are numbered 1/5 (*ortho*), 2/4 (*meta*) and 3 (*para*).





**Fig. 5** Selected hyperconjugative interactions in **B**, representing the transfer of electron density from a Ga-C  $\sigma$  bond (left) and a C-C  $\pi$  bond (right) to antibonding Si-C  $\sigma^*$  orbitals.

least as important for the bond lengths in the heterocycle, as the nature of the substituent. It needs to be kept in mind, however, that for all these cases the differences in bond lengths are comparatively small.

Finally, we were also interested in the actual number of  $\pi$  electrons in the heterocycles of **7** and **B**, as alkyl and silyl substituents should exhibit distinct electron-donating and -withdrawing properties, through their hyperconjugative interactions. The results indicate, however, that there are only minor differences: for **7**, the NBO analysis revealed a total of 5.96 electrons in orbitals contributing to the  $\pi$  density of the heterocycle, compared to 5.89 electrons for **B**. Nucleus-independent chemical shift (NICS)<sup>31</sup> calculations for **7** produced NICS(0) and NICS(1) values of  $-4.8$  and  $-5.9$ , respectively. These numbers differ slightly from the ones reported for **B** ( $-2.4$  and  $-4.4$ ),<sup>13</sup> but suggest a similar aromatic character for both systems.

## Conclusions

Reactions of simple Lewis acids such as  $\text{ECl}_3$  ( $\text{E} = \text{Al}$  and  $\text{Ga}$ ) with rare-earth-metal (Ln) supported aluminata/gallatabenzene complexes give access to new  $\text{E}_3$  multicyclic species. These compounds contain the known anionic heterobenzene-type moiety and hitherto unknown pentadienyl stabilized “bis(heterocyclobutane” cations, as suggested by mass spectroscopy. Metathetical  $\text{Ln} \rightarrow$  metal gallatabenzene transfer is also feasible by exploiting the oxophilic character of the rare-earth element. Applying this strategy, the potassium coordination polymer  $[(1\text{-Me-3,5-}t\text{Bu}_2\text{-C}_5\text{H}_3\text{Ga})\text{K}(\text{THF})]_n$  could be obtained from potassium *tert*-butoxide. Coordinative displacement of the potassium cation with [2.2.2]cryptand generates the separated ion pair  $[(1\text{-Me-3,5-}t\text{Bu}_2\text{-C}_5\text{H}_3\text{Ga})][\text{K}([2.2.2]\text{crypt})]$ . For the unsupported monoanionic gallatabenzene, DFT calculations in combination with a natural bond analysis revealed that a range of hyperconjugative interactions are at play, which help explain the slightly different bonding within the heterocycle, compared to the related silyl-substituted  $[\text{1-Mes-2,6-Si}(\text{iPr}_3)_2\text{-C}_5\text{H}_3\text{Ga}][\text{Li}(\text{dme})_3]$ . Therefore, the observed structural differences should not be over-interpreted in terms of a notable

change in aromaticity. In line with this interpretation, the different nature of the substituents did not afford notable differences in the  $\pi$  electron density for these two systems.

## Author contributions

JL: synthesis and characterization of compounds and writing and editing – original draft; MM: mass spectrometry of compound **3**; CM-M: crystallography and editing – original draft; PS: DFT calculations, and writing and editing – original draft, and funding acquisition; RA: conceptualization, supervision, writing and editing – original draft, project administration, and funding acquisition.

## Conflicts of interest

There are no conflicts to declare.

## Data availability

The data that support the findings of this study are available in the supplementary information (SI). Supplementary information: supporting figures, detailed crystallographic data, spectroscopic data (NMR and IR), and analytical details. See DOI: <https://doi.org/10.1039/d5qi02023a>.

CCDC 2491667–2491671 contain the supplementary crystallographic data for this paper.<sup>32a–e</sup>

## Acknowledgements

We acknowledge support from the State of Baden-Württemberg through bwHPC and the German Research Foundation (DFG) through grant no INST 40/575-1 FUGG (JUSTUS 2 cluster).

## References

- For reviews, see: (a) K. K. Baldrige, O. Uzan and J. M. L. Martin, The silabenzenes: structure, properties, and aromaticity, *Organometallics*, 2000, **19**, 1477–1487; (b) N. Tokitoh, New Progress in the Chemistry of Stable Metallaaromatic Compounds of Heavier Group 14 Elements, *Acc. Chem. Res.*, 2004, **37**, 86–94; (c) P. Cui and Y. Chen, Boratabenzene rare-earth metal complexes, *Coord. Chem. Rev.*, 2016, **314**, 2–13; (d) W. Ma, C. Yu, T. Chen, L. Xu, W.-X. Zhang and Z. Xi, Metallacyclopentadienes: synthesis, structure and reactivity, *Chem. Soc. Rev.*, 2017, **46**, 1160–1192; (e) M. Saito, Transition-metal complexes featuring dianionic heavy group 14 element aromatic ligands, *Acc. Chem. Res.*, 2018, **51**, 160–169; (f) J. Wei, W.-X. Zhang and Z. Xi, The aromatic dianion metalloles, *Chem. Sci.*, 2018, **9**, 560–568; (g) Z. Dong, L. Albers and T. Müller,



Trialkylsilyl-Substituted Silole and Germole Dianions as Precursors for Unusual Silicon and Germanium Compounds, *Acc. Chem. Res.*, 2020, **53**, 532–543; (h) K. Ota and R. Kinjo, Heavier element-containing aromatics of  $[4n + 2]$ -electron systems, *Chem. Soc. Rev.*, 2021, **50**, 10594–10673; (i) D. Schädle and R. Anwander, in *Comprehensive Organometallic Chemistry IV*, ed. G. Parkin, K. Meyer and D. O'Hare, Elsevier, Kidlington, UK, 2022, vol. 4, pp. 1–28; (j) X. Sun and P. W. Roesky, Group 14 metallocle dianions as  $\eta^5$ -coordinating ligands, *Inorg. Chem. Front.*, 2023, **10**, 5509–5516.

2 (a) K. Wakita, N. Tokitoh, R. Okazaki and S. Nagase, Synthesis and Properties of an Overcrowded Silabenzene Stable at Ambient Temperature, *Angew. Chem., Int. Ed.*, 2000, **39**, 634–636; (b) K. Wakita, N. Tokitoh, R. Okazaki, N. Takagi and S. Nagase, Crystal Structure of a Stable Silabenzene and Its Photochemical Isomerization into the Corresponding Silabenzvalene, *J. Am. Chem. Soc.*, 2000, **122**, 5648–5649.

3 (a) N. Nakata, N. Takeda and N. Tokitoh, Synthesis and Properties of the First Stable Germabenzene, *J. Am. Chem. Soc.*, 2002, **124**, 6914–6920; (b) N. Tokitoh, N. Nakata, A. Shinohara, N. Takeda and T. Sasamori, Coordination Chemistry of a Kinetically Stabilized Germabenzene: Syntheses and Properties of Stable  $\eta^6$ -Germabenzene Complexes Coordinated to Transition Metals, *Chem. – Eur. J.*, 2007, **13**, 1856–1862.

4 (a) R. Haga, M. Saito and M. Yoshioka, Reversible Redox Behavior between Stannole Dianion and Distannole-1,2-Dianion, *J. Am. Chem. Soc.*, 2006, **128**, 4934–4935; (b) Y. Mizuhata, T. Sasamori, N. Takeda and N. Tokitoh, A Stable Neutral Stannaromatic Compound: Synthesis, Structure and Complexation of a Kinetically Stabilized 2-Stannanaphthalene, *J. Am. Chem. Soc.*, 2006, **128**, 1050–1051; (c) C. Kaiya, K. Suzuki and M. Yamashita, A Monomeric Stannabenzene: Synthesis, Structure, and Electronic Properties, *Angew. Chem., Int. Ed.*, 2019, **58**, 7749–7752.

5 (a) M. Saito, M. Skaguchi, T. Tajima, K. Ishimura, S. Nagase and M. Hada, Dilithiobplumbole: A Lead-Bearing Aromatic Cyclopentadienyl Analog, *Science*, 2010, **328**, 339–342; (b) M. Saito, T. Akiba, M. Kaneko, T. Kawamura, M. Abe, M. Hada and M. Minoura, Synthesis, Structure, and Reactivity of Lewis Base Stabilized Plumbacyclopentadienylidene, *Chem. – Eur. J.*, 2013, **19**, 16946–16953.

6 (a) C. Krüger, J. C. Sekutowski, H. Hoberg and R. Krause-Göing, (Pentaphenyl)aluminacyclopentadiene as a complexing ligand. The molecular structure of (pentaphenyl)aluminacyclopentadiene and its complex with 1,5-cyclooctadienickel, *J. Organomet. Chem.*, 1977, **141**, 141–148; (b) H. Hoberg, R. Krause-Göing, C. Krüger and J. C. Sekutowski, Novel Organonickel Compounds from (Pentaphenyl)aluminacyclopentadiene, *Angew. Chem., Int. Ed. Engl.*, 1977, **16**, 183–184; (c) H. Hoberg and R. Krause-Göing, Darstellung und Eigenschaften von (Pentaphenyl)aluminacyclopentadiene, *J. Organomet. Chem.*, 1977, **127**, C29–C31.

7 (a) T. Agou, T. Wasano, P. Jin, S. Nagase and N. Tokitoh, Syntheses and Structures of an “Alumole” and Its Dianion, *Angew. Chem., Int. Ed.*, 2013, **52**, 10031–10034; (b) T. Wasano, T. Agou, T. Sasamori and N. Tokitoh, Synthesis, structure and reactivity of a 1-bromoalumole, *Chem. Commun.*, 2014, **50**, 8148–8150.

8 (a) A. Decken, F. P. Gabbai and A. H. Cowley, The Benzannelation Approach to Novel Gallium and Indium Heterocycles, *Inorg. Chem.*, 1995, **34**, 3853–3854; (b) A. H. Cowley, D. S. Brown, A. Decken and S. Kamepalli, Novel dimeric ring systems containing gallium, *Chem. Commun.*, 1996, 2425–2426.

9 P. Wei, X.-W. Li and G. H. Robinson,  $[\text{Ga}_2\text{Cl}_4(\text{dioxane})_2]_x$ : molecular structure and reactivity of a polymeric gallium(II) halide containing two five-coordinate gallium atoms about a Ga–Ga bond, *Chem. Commun.*, 1999, 1287–1288.

10 T. Agou, T. Wasano, T. Sasamori and N. Tokitoh, Syntheses and structures of a stable gallole free of Lewis base coordination and its dianion, *J. Phys. Org. Chem.*, 2015, **28**, 104–107.

11 A. J. Ashe III, S. Al-Ahmad and J. W. Kampf, Aromatic Gallium Heterocycles: Synthesis of the First Gallabenzene, *Angew. Chem., Int. Ed. Engl.*, 1995, **34**, 1357–1359.

12 (a) T. Nakamura, K. Suzuki and M. Yamashita, An Anionic Aluminabenzene Bearing Aromatic and Ambiphilic Contributions, *J. Am. Chem. Soc.*, 2014, **136**, 9276–9279; (b) T. Nakamura, K. Suzuki and M. Yamashita, Aluminabenzene–Zirconium Complexes: Intramolecular Coordination of Chloride to Aluminum, *Organometallics*, 2015, **34**, 813–816; (c) T. Nakamura, K. Suzuki and M. Yamashita, Aluminabenzene–Rh and –Ir Complexes: Synthesis, Structure, and Application toward Catalytic C–H Borylation, *J. Am. Chem. Soc.*, 2017, **139**, 17763–17766; (d) T. Nakamura, K. Suzuki and M. Yamashita, Zwitterionic Aluminabenzene–Alkylzirconium Complex Having Half-Zirconocene Structure: Synthesis and Application for an Additive-Free Ethylene Polymerization, *Chem. Commun.*, 2018, **54**, 4180–4183.

13 T. Nakamura, K. Suzuki and M. Yamashita, An Isolable Anionic Gallabenzene: Synthesis and Characterization, *Organometallics*, 2015, **34**, 1806–1808.

14 T. Nakamura, K. Suzuki and M. Yamashita, Anionic Indabenzene: synthesis and characterization, *Chem. Commun.*, 2017, **53**, 13260–13263.

15 J. Raeder, M. Reiners, R. Baumgarten, K. Münster, D. Baabe, M. Freytag, P. G. Jones and M. D. Walter, Synthesis and molecular structure of pentadienyl complexes of the rare-earth metals, *Dalton Trans.*, 2018, **47**, 14468–14482.

16 (a) D. Barisic, D. Schneider, C. Maichle-Mössmer and R. Anwander, Formation and Reactivity of an Aluminabenzene Ligand at Pentadienyl-Supported Rare-Earth Metals, *Angew. Chem., Int. Ed.*, 2019, **58**, 1515–1518;

(b) D. Barisic, D. A. Buschmann, D. Schneider, C. Maichle-Mössmer and R. Anwander, Rare-Earth Metal Pentadienyl Half-Sandwich and Sandwich Tetramethylaluminates – Synthesis, Structure, Reactivity, and Performance in Isoprene Polymerization, *Chem. – Eur. J.*, 2019, **25**, 4821–4832; (c) D. Barisic, J. Lebon, C. Maichle-Mössmer and R. Anwander, Pentadienyl migration and abstraction in yttrium aluminabenzene complexes including a single-component catalyst for isoprene polymerization, *Chem. Commun.*, 2019, 7089–7092.

17 (a) J. Lebon, D. Barisic, C. Maichle-Mössmer and R. Anwander, Yttrium Complexes with Group 13 Heterobenzene-type Ligands, *Chem. – Eur. J.*, 2023, **29**, e202302846; (b) J. Lebon, M. Beauvois, C. Maichle-Mössmer, P. Sirsch and R. Anwander, Gallatabenzene Ligands Emerging from Open Lutetocene and Yttrocene Methyl Complexes, *Chem. – Eur. J.*, 2024, **30**, e202403472.

18 Other examples of pentadienyl cyclometallation: (a) M. S. Kralik, J. P. Hutchinson and R. D. Ernst, New Carbon–Carbon Bond-Forming Reaction of Carbon Monoxide: Remarkable Trialkylation of a Carbonyl Ligand in a Molybdenum Pentadienyl Complex, *J. Am. Chem. Soc.*, 1985, **107**, 8296–8297; (b) M. S. Kralik, A. L. Rheingold and R. D. Ernst, (Pentadienyl)molybdenum Carbonyl Chemistry: Conversion of a Pentadienyl Ligand to a Coordinated Metallabenzene Complex, *Organometallics*, 1987, **6**, 2612–2614; (c) J. R. Bleeke, Y.-F. Xie, W.-J. Peng and M. Chiang, Metallabenzene: Synthesis, Structure, and Spectroscopy of a 1-Irida-3,5-dimethylbenzene Complex, *J. Am. Chem. Soc.*, 1989, **111**, 4118–4120; (d) J. R. Bleeke and W.-J. Peng, Synthesis, Structure, and Spectroscopy of Iridacyclohexadiene Complexes, *Organometallics*, 1987, **6**, 1576–1578; (e) J. R. Bleeke, Metallabenzene Chemistry, *Acc. Chem. Res.*, 1991, **24**, 271–277; (f) M. S. Kralik, L. Stahl, A. M. Arif, C. E. Strouse and R. D. Ernst, Open and Half-Open Manganocene Chemistry: More Associated Salts, *Organometallics*, 1992, **11**, 3617–3621; (g) U. Effertz, U. Englert, F. Podewils, A. Salzer, T. Wagner and M. Kaupp, Reaction of Pentadienyl Complexes with Metal Carbonyls: Synthetic, Structural, and Theoretical Studies of Metallabenzene  $\pi$ -Complexes, *Organometallics*, 2003, **22**, 264–274; (h) U. Bertling, U. Englert and A. Salzer, From Triple-Decker to Metallabenzene: A New Generation of Sandwich Complexes, *Angew. Chem., Int. Ed. Engl.*, 1994, **33**, 1003–1004; (i) U. Englert, F. Podewils, I. Schifflers and A. Salzer, The First Homoleptic Metallabenzene Sandwich Complex, *Angew. Chem., Int. Ed.*, 1998, **37**, 2134–2136.

19 M. H. Dietrich, K. W. Törnroos, E. Herdtweck and R. Anwander, Tetramethylaluminate and Tetramethylgallate Coordination in Rare-Earth Metal Half-Sandwich and Metallocene Complexes, *Organometallics*, 2009, **28**, 6739–6749.

20 (a) W. J. Evans, J. W. Grate, K. R. Levan, I. Bloom, T. T. Peterson, R. J. Doedens, H. Zhang and J. L. Atwood, Synthesis and X-ray Crystal Structure of Bis(pentamethylcyclopentadienyl) Lanthanide and Yttrium Halide Complexes, *Inorg. Chem.*, 1986, **25**, 3614–3619; (b) W. J. Evans, T. T. Peterson, M. D. Rausch, W. E. Hunter, H. Zhang and J. L. Atwood, Synthesis and X-ray Crystallographic Characterization of an Asymmetric Organoyttrium Halide Dimer:  $(C_5Me_5)_2Y(\mu-Cl)YCl(C_5Me_5)_2$ , *Organometallics*, 1985, **3**, 554–559.

21 W. Uhl, Hydroalumination and hydrogallation of alkynes: New insights into the course of well-known reactions, *Coord. Chem. Rev.*, 2008, **252**, 1540–1563.

22 W. Uhl, A. Vinogradov and S. Grimme, C–H Bond Activation by Hyperconjugation with Al–C Bonds and by Chelating Coordination of the Hydride Ion, *J. Am. Chem. Soc.*, 2007, **129**, 11259–11264.

23 A. Brand, A. Hepp, E.-U. Würthwein and W. Uhl, Tridentate Ligand with Three Carbanions as Donor Atoms: Formation of Dinuclear, Heptacyclic Complexes of Boron, Aluminum, or Gallium with B–C–B, Al–C–Al, or Ga–C–Ga Three-Center–Two-Electron Bonds, *Organometallics*, 2020, **59**, 5558–5563.

24 S. G. Bott, A. Alvanipour, S. D. Morley, D. A. Atwood, C. M. Means, A. W. Coleman and J. L. Atwood, Stabilization of the  $[AlMe_2]^+$  Cation by Crown Ethers, *Angew. Chem., Int. Ed. Engl.*, 1987, **26**, 485–486.

25 W. Uhl, J. Wagner, D. Fenske and G. Baum, N,N,N',N'-tetramethylethylenediamin-di(*tert*-butyl)aluminium-Kationen – Molekülstruktur des  $[(Me_3C)_2Al\text{-TMEDA}]^+[(Me_3C)_2Al\text{ Br}_2]^-$ , *Z. Anorg. Allg. Chem.*, 1992, **612**, 25–34.

26 W. Uhl, L. Cuypers, B. Neumüller and F. Weller, Hydrogallation of Alkynes: Syntheses of Carbon–Gallium Cages Possessing Heteroadamantane Structures, *Organometallics*, 2002, **21**, 2365–2368.

27 Y. Mizuhata, S. Fujimori, T. Sasamori and N. Tokitoh, Germabenzenylpotassium: A Germanium Analogue of a Phenyl Anion, *Angew. Chem., Int. Ed.*, 2017, **56**, 4588–4592.

28 M. J. Frisch, G. W. Trucks, H. B. Schlegel, G. E. Scuseria, M. A. Robb, J. R. Cheeseman, G. Scalmani, V. Barone, G. A. Petersson, H. Nakatsuji, X. Li, M. Caricato, A. V. Marenich, J. Bloino, B. G. Janesko, R. Gomperts, B. Mennucci, H. P. Hratchian, J. V. Ortiz, A. F. Izmaylov, J. L. Sonnenberg, D. Williams-Young, F. Ding, F. Lipparini, F. Egidi, J. Goings, B. Peng, A. Petrone, T. Henderson, D. Ranasinghe, V. G. Zakrzewski, J. Gao, N. Rega, G. Zheng, W. Liang, M. Hada, M. Ehara, K. Toyota, R. Fukuda, J. Hasegawa, M. Ishida, T. Nakajima, Y. Honda, O. Kitao, H. Nakai, T. Vreven, K. Throssell, J. A. Montgomery Jr., J. E. Peralta, F. Ogliaro, M. J. Bearpark, J. J. Heyd, E. N. Brothers, K. N. Kudin, V. N. Staroverov, T. A. Keith, R. Kobayashi, J. Normand, K. Raghavachari, A. P. Rendell, J. C. Burant, S. S. Iyengar, J. Tomasi, M. Cossi, J. M. Millam, M. Klene, C. Adamo, R. Cammi, J. W. Ochterski, R. L. Martin, K. Morokuma, O. Farkas, J. B. Foresman and D. J. Fox, *Gaussian 16, Revision C.01*, Gaussian, Inc., Wallingford CT, 2019.

29 C. R. Landis and F. Weinhold, in *The Chemical Bond: Fundamental Aspects of Chemical Bonding* Weinheim, ed. G. Frenking and S. Shaik, Wiley-VCH, Germany, 2014, pp. 91–120.

30 V. Pophristic and L. Goodman, Hyperconjugation not steric repusion leads to staggered structure of ethane, *Nature*, 2001, **411**, 565–568.

31 Z. Chen, C. S. Wannere, C. Corminboeuf, R. Puchta and P. v. R. Schleyer, Nucleus-Independent Chemical Shifts (NICS) as an Aromaticity Criterion, *Chem. Rev.*, 2005, **105**, 3842–3888.

32 (a) CCDC 2491667: Experimental Crystal Structure Determination, 2025, DOI: [10.5517/ccdc.csd.cc2pmsch](https://doi.org/10.5517/ccdc.csd.cc2pmsch);  
(b) CCDC 2491668: Experimental Crystal Structure Determination, 2025, DOI: [10.5517/ccdc.csd.cc2pmsdj](https://doi.org/10.5517/ccdc.csd.cc2pmsdj);  
(c) CCDC 2491669: Experimental Crystal Structure Determination, 2025, DOI: [10.5517/ccdc.csd.cc2pmsfk](https://doi.org/10.5517/ccdc.csd.cc2pmsfk);  
(d) CCDC 2491670: Experimental Crystal Structure Determination, 2025, DOI: [10.5517/ccdc.csd.cc2pmsgl](https://doi.org/10.5517/ccdc.csd.cc2pmsgl);  
(e) CCDC 2491671: Experimental Crystal Structure Determination, 2025, DOI: [10.5517/ccdc.csd.cc2pmshm](https://doi.org/10.5517/ccdc.csd.cc2pmshm).